Deeply Bound 1*s* and 2*p* Pionic States in ^{205}Pb and Determination of the *s*-Wave Part of the Pion-Nucleus Interaction

H. Geissel,[1] H. Gilg,[2] A. Gillitzer,[3] R. S. Hayano,[4] S. Hirenzaki,[5] K. Itahashi,[6] M. Iwasaki,[6] P. Kienle,[2] M. Münch,[2] G. Münzenberg,[1] W. Schott,[2] K. Suzuki,[4] D. Tomono,[6] H. Weick,[1] T. Yamazaki,[7] and T. Yoneyama[6]

[1]*Gesellschaft für Schwerionenforschung, D-64291 Darmstadt, Germany*
[2]*Physik-Department, Technische Universität München, D-85747 Garching, Germany*
[3]*Institut für Kernphysik, Forschungszentrum Jülich, D-52425 Jülich, Germany*
[4]*Department of Physics, University of Tokyo, 7-3-1 Hongo, Bunkyo-ku, Tokyo 113-0033, Japan*
[5]*Department of Physics, Nara Women's University, Kita-Uoya, Nishimachi, Nara 630-8506, Japan*
[6]*Department of Physics, Tokyo Institute of Technology, 2-12-1 Ookayama, Meguro-ku, Tokyo 152-8551, Japan*
[7]*RI Beam Science Laboratory, RIKEN, 2-1 Hirosawa, Wako-shi, Saitama 351-0198, Japan*

We observed well-separated 1*s* and 2*p* π^- states in ^{205}Pb in the ^{206}Pb$(d, {}^3$He$)$ reaction at $T_d = 604.3$ MeV. The binding energies and the widths determined are $B_{1s} = 6.762 \pm 0.061$ MeV, $\Gamma_{1s} = 0.764^{+0.171}_{-0.154}$ MeV, $B_{2p} = 5.110 \pm 0.045$ MeV, and $\Gamma_{2p} = 0.321^{+0.060}_{-0.062}$ MeV. They are used to deduce the real and imaginary strengths of the *s*-wave part of the pion-nucleus interaction, which translates into a positive mass shift of π^- in ^{205}Pb.

In a recent experiment at GSI, we have discovered the deeply bound 2*p* state and an indication of the 1*s* state of negative pions in ^{207}Pb in the ^{208}Pb$(d, {}^3$He$)$ reaction [1–4]. This experiment has demonstrated that (i) the deeply bound π^- states (1*s* and 2*p*) in heavy nuclei indeed exist with narrow widths and that (ii) they are produced in the $(d, {}^3$He$)$ reaction, as theoretically predicted [5–8]. The narrowness of these deeply bound states despite the strong pion absorption in nuclei is well understood as being due to the halolike pionic structure, which is accommodated in a potential pocket provided by the long-range Coulomb attraction and the short-range nuclear repulsion [5,6,9]. The $(d, {}^3$He$)$ reaction produces deeply bound states of configurations $(nl)_\pi(n'l'_{j'})^{-1}_n$ at small momentum transfer. The observed spectrum in the previous experiment showed a distinct but skewed $(2p)_\pi$ peak due to the presence of the $3p_{1/2}$ and $3p_{3/2}$ neutron hole states separated in energy by 0.90 MeV. The $(1s)_\pi$ state was observed as a bump at the shoulder of the $(2p)_\pi$ peak accordingly. In the present paper, we report on a new experiment using a ^{206}Pb target, which was purposely undertaken in view of the smaller contribution of the $3p_{1/2}$ hole and, consequently, a better separation of the $(1s)_\pi$ and $(2p)_\pi$ states. This expectation was supported by a theoretical study [10].

The experiment was performed with the Fragment Separator (FRS) [11] using a $T_d = 604.3$ MeV deuteron beam from the SIS-18 synchrotron at GSI, Darmstadt. The detailed description of the experimental procedures and analyses are found in Refs. [3,4,12]. The beam intensity was 1.5×10^{11}/spill at 1 s spill duration and 3 s cycle time. We employed a 1.5 mm wide and 25 mg/cm^2 thick ^{206}Pb target. The ^{3}He momentum spectrum was measured at excitation energies covering the bound π^- region.

The obtained excitation spectrum, namely, the double differential cross section versus the excitation energy (E_x) above the ground state of ^{205}Pb, is shown in Fig. 1. The excitation energy of a bound-pion peak is related to the π^- binding energy B_{nl} as $E_x = [M_x - M(^{205}$Pb$)]c^2 = m_{\pi^-}c^2 - B_{nl} + E_n(n'l'_{j'})$, where M_x is the mass of the reaction product, $M(^{205}$Pb$)$ is the ground-state mass of ^{205}Pb, $m_{\pi^-} = 139.570$ MeV/c^2 is the pion mass, and $E_n(n'l'_{j'})$ is the excitation energy of ^{205}Pb (neutron hole
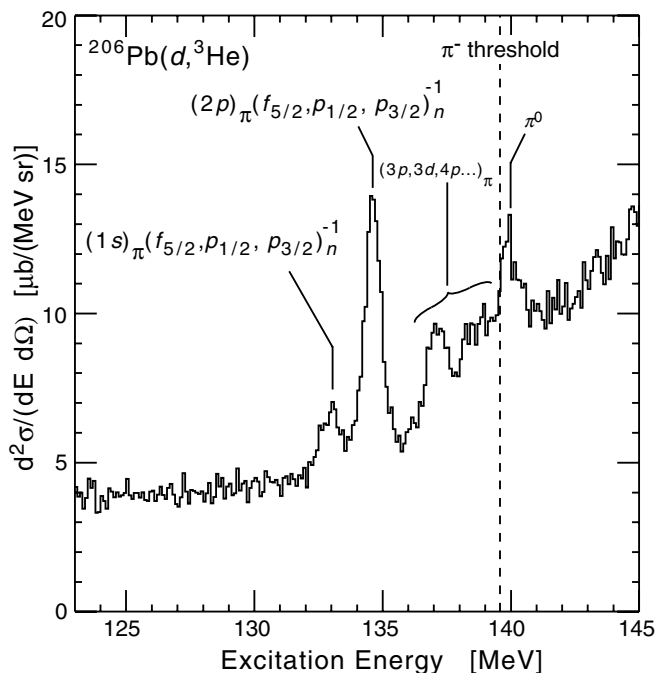

FIG. 1. Double differential cross section measured in the ^{206}Pb$(d, {}^3$He$)$ reaction at incident deuteron energy $T_d = 604.3$ MeV as a function of the excitation energy above the ^{205}Pb ground state. The peak at 140 MeV designated as "π^0" is due to the reaction $p(d, {}^3$He$)\pi^0$.

state of ^{206}Pb [13]). The most important contributions are from the ground state ($2f_{5/2}$), the 0.002 MeV state ($3p_{1/2}$), the 0.260 MeV state ($3p_{3/2}$), and the 1.770 MeV state ($2f_{7/2}$).

The spectrum consists of three contributions, which originate from (i) quasifree pion production, (ii) formation of bound pionic states, and (iii) nonpionic nuclear excitation. The quasifree π^- production forms a continuum which opens above the emission threshold at $E_x = 139.570$ MeV shown by the vertical dashed line. The peak above the π^- threshold at $E_x \simeq 140$ MeV results from the $p(d, {}^3\text{He})\pi^0$ reaction on a small hydrogen contamination in the target. Nuclear excitation processes not associated with pion production contribute at a nearly constant level $d^2\sigma/(dEd\Omega) \simeq 4 \ \mu b/(\text{MeV sr})$ in the considered excitation energy range, and dominate at $E_x < 130$ MeV. The central part between 130 and 140 MeV has structures associated with the formation of pionic states. The largest peak at $E_x = 135$ MeV corresponds to the bound $(2p)_\pi$ state coupled dominantly to the three neutron hole states $(2f_{5/2}, 3p_{1/2}, 3p_{3/2})_n^{-1}$. The well-separated peak at $E_x \sim 133$ MeV below the $(2p)_\pi$ peak is $(1s)_\pi$, which is also composed of contributions from the three hole states. The region between the $(2p)_\pi$ peak and the threshold ($E_x = 136 \sim 139$ MeV) is due to the formation of higher states $(3p, 3d, 4p, \ldots)_\pi$. The overall structure agrees remarkably well with the theoretical one [10]. The experimental resolution and the uncertainty in the absolute energy scale are estimated to be 0.374 ± 0.050 MeV (FWHM) and 0.040 MeV, respectively (see Ref. [12]).

In order to determine the binding energies and widths, we decomposed the region of interest (see Fig. 2) into $(1s)_\pi$ and $(2p)_\pi$ components and a linear background by a least squares fit in a similar manner as in Ref. [4]. The fitting region is between $E_x = 120.0$ and 136.2 MeV where the contribution from states other than $(1s)_\pi$ and $(2p)_\pi$ is negligible. In the final analysis each pionic state $(nl)_\pi$ is coupled to ten neutron hole states with calculated strengths as listed in Table II of Ref. [10]. The fitting parameters are the binding energies (B_{nl}), widths (Γ_{nl}), and intensities (I_{nl}) of both $(1s)_\pi$ and $(2p)_\pi$, and the slope and the offset of the linear background. The result of this fitting is excellent (the χ^2 is 98.0 for $N_{\text{DF}} = 124$), but we find a small discrepancy near the tiny structure of $(2p)_\pi(2f_{7/2})_n^{-1}$ at ~ 136.2 MeV, although this is located mostly outside the fitting region. A 40% reduction of the f-hole contributions, $(2f_{5/2}$ and $2f_{7/2})_n^{-1}$, compared with the theoretical ones removes this discrepancy, and yields binding energies B_{1s} and B_{2p} which are slightly larger by 0.024 and 0.026 MeV, respectively (the χ^2 is 93.1 for $N_{\text{DF}} = 123$). The fit result of this option is shown in Fig. 2a. In the interval 130 MeV $< E_x <$ 136 MeV, the solid curve shows the obtained fit function, and the dashed and the dotted curves are the $(1s)_\pi$ and $(2p)_\pi$ contributions, respectively. The peak intensity of $(1s)_\pi$ relative to $(2p)_\pi$ is 73% larger than the theoretical prediction. The contributions of the
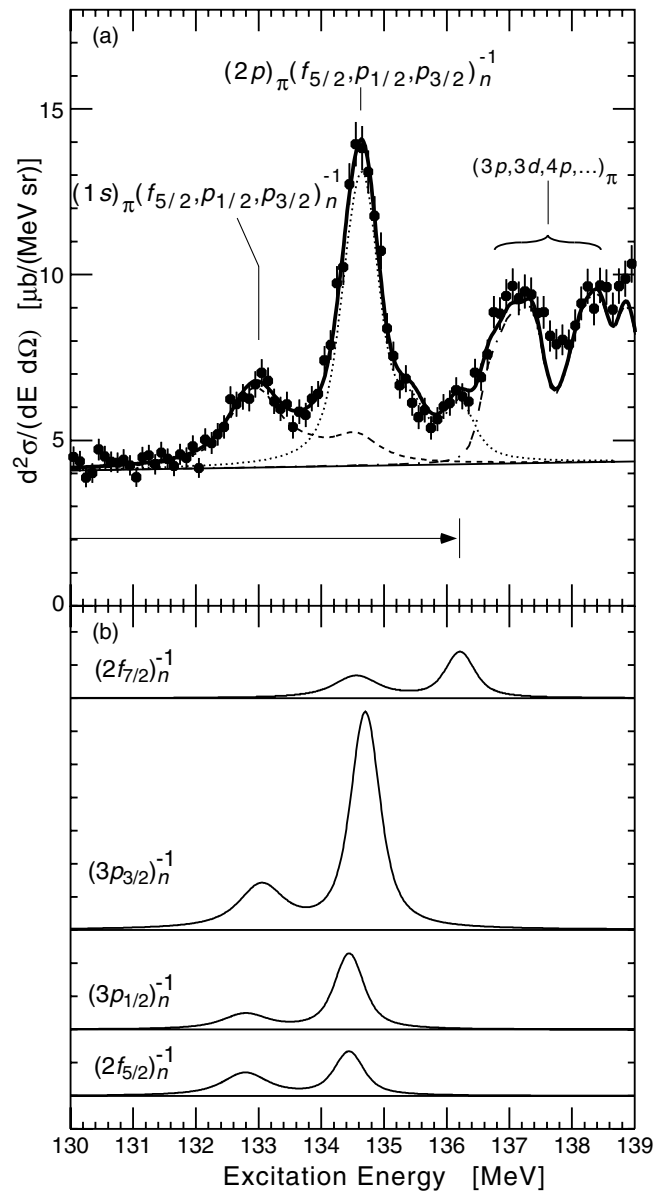

FIG. 2. (a) The experimental spectrum and the best fit curve obtained in the fit region indicated by the horizontal arrow. The dashed, dotted, and dash-dotted curves are the $(1s)_\pi$, $(2p)_\pi$, and higher-$(nl)_\pi$ components, respectively. (b) The partial contributions of the most dominant neutron hole states, shown in the same scale as (a).

shallower states $(3p, 3d, 4p, \ldots)_\pi$ were not considered in the fitting procedure because they are located outside the region relevant for the deduction of the $(1s)_\pi$ and $(2p)_\pi$ binding energies and widths. Using the theoretical values from Ref. [10] for the relative strength of the shallower states as compared to the $(2p)_\pi$ state, their summed contribution was obtained, as presented by the dash-dotted curve. This contribution is included in the solid curve in addition to the fit function in order to demonstrate that the excitation spectrum is well understood also in the region of shallow bound pionic states.

The deduced binding energies and widths are presented in Table I, where we adopt the average values resulting from the two fit options described above. The systematic uncertainties due to the choice of the f-hole contribution are ± 0.012 and ± 0.013 MeV for B_{1s} and B_{2p}, respectively. The systematic errors are obtained from a quadratic sum of the evaluated uncertainties, which are dominated by the uncertainty of the absolute energy scale for B and by the uncertainty of the experimental resolution for Γ. The present values are much more precise than the former ones obtained for $\pi^- \otimes {}^{207}\text{Pb}$ [4].

In Fig. 3 the experimental data are presented in the B-Γ planes with the 1σ contours for the statistical errors and with the bars for the total (statistical + systematic) errors. Here we compare the experimental results with those calculated by using a pion-nucleus potential of the Ericson-Ericson type [14] with various potential parameter sets which were obtained from fitting observed strong interaction shifts and widths in pionic atoms (see Refs. [4,15,16]). The pion-nucleus potential consists of the s-wave (local) part (U_s) and the p-wave (nonlocal) part (U_p). Whereas the known strong interaction shifts in most of the shallow states in pionic atoms are due to the combination of attractive U_p and repulsive U_s terms, the $(1s)_\pi$ states are dominated by the s-wave part (see Fig. 1 of Ref. [17]). This part is given by

$$U_s(r) = -\frac{2\pi}{m_\pi}[\epsilon_1\{b_0\rho(r) + b_1\Delta\rho(r)\} + \epsilon_2 B_0\rho^2(r)], \tag{1}$$

where $\rho(r) = \rho^{(n)}(r) + \rho^{(p)}(r)$, $\Delta\rho(r) = \rho^{(n)}(r) - \rho^{(p)}(r)$, $\epsilon_1 = 1 + m_\pi/M = 1.147$, and $\epsilon_2 = 1 + m_\pi/2M = 1.073$ with M being the nucleon mass. We assumed the two-parameter Fermi distributions for the neutron density $\rho^{(n)}(r)$ and the proton density $\rho^{(p)}(r)$ with a common nuclear radius $c_p = c_n = 6.591$ fm and a diffuseness parameter $z_p = z_n = 0.545$ fm for ^{205}Pb, which are taken as the average of the proton parameters for ^{204}Pb and ^{206}Pb [18]. The central densities for neutrons [$\rho^{(n)}(0)$] and protons [$\rho^{(p)}(0)$] are 0.0961 and

TABLE I. The binding energies and widths of the $(1s)_\pi$ and $(2p)_\pi$ states of ^{205}Pb obtained in the present experiment.

$B_{1s} = 6.762$	± 0.061	$[\pm 0.045 \text{ (stat)} \pm 0.041 \text{ (syst)}]$ MeV
$\Gamma_{1s} = 0.764$	$^{+0.171}_{-0.154}$	$[^{+0.162}_{-0.141} \text{ (stat)} \pm {}^{+0.055}_{-0.061} \text{ (syst)}]$ MeV
$B_{2p} = 5.110$	± 0.045	$[\pm 0.016 \text{ (stat)} \pm 0.042 \text{ (syst)}]$ MeV
$\Gamma_{2p} = 0.321$	$^{+0.060}_{-0.062}$	$[\pm 0.039 \text{ (stat)} \pm {}^{+0.045}_{-0.049} \text{ (syst)}]$ MeV

0.0640 fm^{-3}, respectively. The calculated values of B and Γ, for which the effect of vacuum polarization is taken into account, are shown in Fig. 3. Most of them are in fair agreement with the experimental values, though the individual potential parameters are widely distributed.

Conversely, we determine the strengths of the real and the imaginary parts of the s-wave potential, $U_s(r) = V(r) + iW(r)$, irrespective to the choice of the p-wave parameters, since the $(1s)_\pi$ binding energy and width depend nearly entirely on the s-wave potential. The well-established Seki-Masutani relation [4,6,19], $b_0^* \approx b_0 + \frac{\epsilon_2}{\epsilon_1}\frac{\rho(0)}{2}\text{Re}B_0 \approx$ const, further implies that the real part of the potential is well represented by its value at the half-density radius R_0.

The theoretical relations of B_{1s} and Γ_{1s} with V_0^* [$\equiv 2V(R_0)$] and $-W(0)$ obtained in this way, while setting the insensitive p-wave parameters to the well-known values [15,19], are presented as two-dimensional contour curves in Fig. 4. The width depends not only on the imaginary part but also on the real part through the overlap of the π^- density with the nucleus. The binding energy depends also on the imaginary part. The experimental values of B_{1s} and Γ_{1s} presented in the figure yield

$$V_0^* = 2V(R_0) = 27.1 \pm 1.7 \text{ MeV}, \tag{2}$$

$$W(0) = -14.0 \pm 3.8 \text{ MeV}. \tag{3}$$

Thus far, we have assumed that the shapes of $\rho^{(p)}(r)$ and $\rho^{(n)}(r)$ are the same. If the rms radius of the neutron distribution is larger than that of the proton distribution [20], it would cause a decrease in the calculated $1s$ binding energy [17,21], which results in a decrease of V_0^* by about 2 MeV.
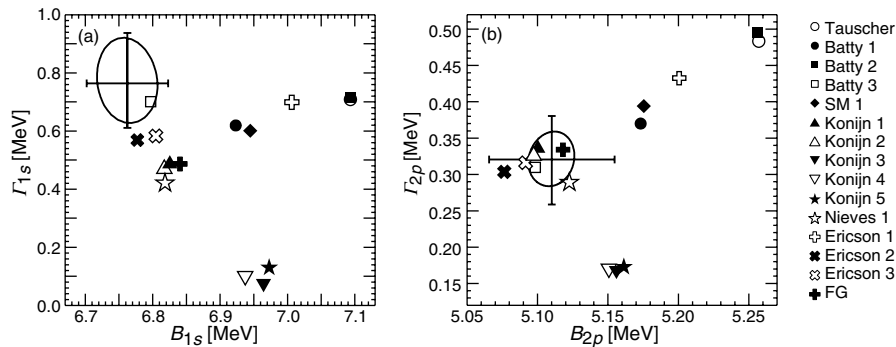

FIG. 3. Comparison of the measured binding energy and width for (a) $(1s)_\pi$ and (b) $(2p)_\pi$ in ^{205}Pb with the corresponding values calculated by using various potential parameter sets (abbreviated as in [4] except for FG [16]). When necessary, an isotope shift of $B_{1s}(^{205}\text{Pb}) \sim B_{1s}(^{207}\text{Pb}) + 40.5$ keV is applied. The small ellipses and the bars show the experimental values with 1σ statistical and total (statistical + systematic) errors, respectively.
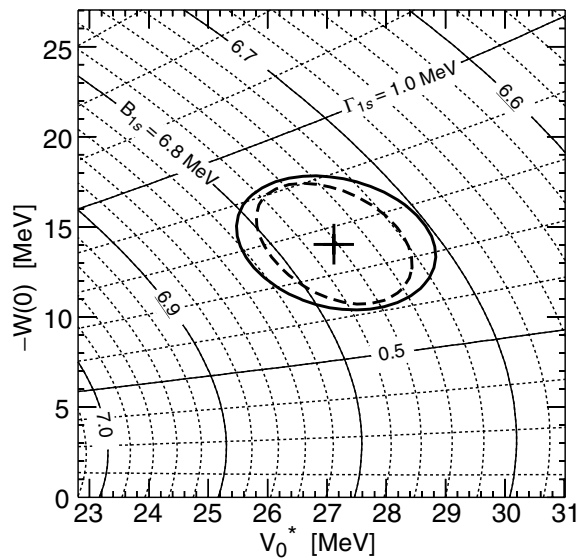
FIG. 4. A contour map of B_{1s} and Γ_{1s} in the plane of V_0^* [$= 2V(R_0)$] and $-W(0)$. The experimental values with 1σ statistical and total (statistical + systematic) errors are shown by the broken and solid ellipses, respectively.

The real s-wave potential $V(r)$ translates into an increase of the effective mass of π^- in the nuclear medium [2,22]. The value of V_0^* (~ 27 MeV) corresponds to a pion mass shift in the medium of ^{205}Pb, as the half-density value $V(R_0)$ is extrapolated to the full-density limit $2V(R_0)$. (Strictly speaking, the potential at $r = 0$ is not V_0^* but $V_0^* - (\pi/m_\pi)\epsilon_2 \mathrm{Re}B_0\rho(0)^2$, and thus the pion mass shift *at the center of the nucleus* may have an ambiguity as much as 2–8 MeV, if $\mathrm{Re}B_0 = -0.05 \pm 0.03$ is invoked [16].) It is to be noted that the measured repulsive potential V_0^* is significantly larger than $V_0^* \sim 16$ MeV, which we expect from the free πN scattering lengths after the correction for double scattering ($b_0 = -0.017$ and $b_1 = -0.090$) [14,23]. The difference between the observed value (27 MeV) and the expected value (16 MeV) can be attributed either to an additional isoscalar repulsion [the $\mathrm{Re}B_0\rho(r)^2$ term], as claimed in [16], or to a repulsion due to an increase of the isovector strength $|b_1|$ in the nuclear medium. Such an increase of $|b_1|$ is expected as a consequence of the partial restoration of chiral symmetry at finite nuclear density along with a reduction of the chiral order parameter f_π (or the quark condensate) [24,25]. Further studies of pionic $1s$ states in various Sn isotopes to distinguish between the two interpretations are in progress.

[1] T. Yamazaki *et al.,* Z. Phys. A **355**, 219 (1996).
[2] T. Yamazaki *et al.,* Phys. Lett. B **418**, 246 (1998).
[3] H. Gilg *et al.,* Phys. Rev. C **62**, 025201 (2000).
[4] K. Itahashi *et al.,* Phys. Rev. C **62**, 025202 (2000).
[5] H. Toki and T. Yamazaki, Phys. Lett. B **213**, 129 (1988).
[6] H. Toki, S. Hirenzaki, T. Yamazaki, and R. S. Hayano, Nucl. Phys. **A501**, 653 (1989).
[7] H. Toki, S. Hirenzaki, and T. Yamazaki, Nucl. Phys. **A530**, 679 (1991).
[8] S. Hirenzaki, H. Toki, and T. Yamazaki, Phys. Rev. C **44**, 2472 (1991).
[9] E. Friedman and G. Soff, J. Phys. G **11**, L37 (1985).
[10] S. Hirenzaki and H. Toki, Phys. Rev. C **55**, 2719 (1997).
[11] H. Geissel *et al.,* Nucl. Instrum. Methods Phys. Res., Sect. B **70**, 286 (1992).
[12] K. Suzuki, Master thesis, University of Tokyo, 2000.
[13] R. Tickle and J. Bardwick, Phys. Rev. **178**, 2006 (1969).
[14] M. Ericson and T. E. O. Ericson, Ann. Phys. (N.Y.) **36**, 323 (1966); T. E. O. Ericson and W. Weise, *Pions and Nuclei* (Oxford Science Publications, New York, 1988).
[15] C. Batty, E. Friedman, and A. Gal, Phys. Rep. **287**, 385 (1997).
[16] E. Friedman and A. Gal, Phys. Lett. B **432**, 235 (1998).
[17] Y. Umemoto, S. Hirenzaki, K. Kume, and H. Toki, Phys. Rev. C **62**, 024606 (2000).
[18] H. de Vries, C. W. de Jager, and C. de Vries, At. Data Nucl. Data Tables **36**, 495 (1987).
[19] R. Seki and K. Masutani, Phys. Rev. C **27**, 2799 (1983).
[20] A. Trzcińska, J. Jastrzębski, P. Lubiński, F. J. Hartmann, R. Schmidt, T. von Egidy, and B. Kłos, Acta Phys. Pol. B **32**, 917 (2001); (unpublished).
[21] H. Toki, S. Hirenzaki, and T. Yamazaki, Phys. Lett. B **249**, 391 (1990).
[22] T. Waas, R. Brockman, and W. Weise, Phys. Lett. B **405**, 415 (1997).
[23] T. E. O. Ericson, B. Loiseau, and A. W. Thomas, Nucl. Phys. **A684**, 380 (2001).
[24] W. Weise, Acta Phys. Pol. B **31**, 2715 (2000).
[25] P. Kienle and T. Yamazaki, Phys. Lett. B **514**, 1 (2001).